Directed evolution's selective use of quantum tunneling in designed enzymes – a combined theoretical experimental study

DOI:
10.1021/acs.jpcb.4c08169

Document Version
Accepted author manuscript

Directed evolution's selective use of quantum tunneling in designed enzymes – a combined theoretical experimental study

Kseniia Korchagina[1], Sree Ganesh Balasubramani[2], Jordan Berreur[3], Emilie F. Gerard[3], Linus O. Johannissen[3], Anthony P. Green[3], Sam Hay[3], Steven D. Schwartz[1*]

[1] Department of Chemistry and Biochemistry, University of Arizona, 1306 E University Blvd, Tucson, 85721, Arizona, USA.

2 Quantitative Biosciences Institute, University of California, 1700 4th St, San Francisco, 94158, California, USA.

3 Manchester Institute of Biotechnology and Department of Chemistry, The University of Manchester, 131 Princess Street, Manchester, M1 7DN, UK.

*Corresponding author(s). E-mail(s): sschwartz@arizona.edu;
Contributing authors: kkorchagina@arizona.edu; sreeuci@gmail.com

KEYWORDS: Morita-Baylis-Hillman (MBH) reaction, molecular dynamics, centroid dynamics, transition path sampling, free energy, hydrogen quantum tunneling, kinetic isotope effect.

ABSTRACT: Natural enzymes are powerful catalysts, reducing the apparent activation energy for reaction, enabling chemistry to proceed as much as 10^{15} times faster than the corresponding solution reaction. It has been suggested for some time that in some cases quantum tunneling can contribute to this rate enhancement by offering pathways through a barrier inaccessible to activated events. A central question of interest to both physical chemists and biochemists is the extent to which evolution introduces below the barrier or tunneling mechanisms. In view of the rapidly expanding chemistries for which artificial enzymes have now been created, it is of interest to see how quantum tunneling has been used in these reactions. In this paper, we study the evolution of possible proton tunneling during C-H bond cleavage in enzymes that catalyze the Morita-Baylis-Hillman (MBH) reaction. The enzymes were generated by theoretical design followed by laboratory evolution. We employ classical and centroid molecular dynamics approaches in path sampling computations to determine if there is a quantum contribution to lowering the free energy of the proton transfer for various experimentally generated protein and substrate combinations. This data is compared to experiments reporting on the observed kinetic isotope effect (KIE) for the relevant reactions. Our results indicate modest involvement of tunneling when laboratory evolution has resulted in a system with a higher classical free energy barrier to chemistry (that is when optimization of processes other than chemistry result in a higher chemical barrier.)

INTRODUCTION

Certain reactions of importance in organic synthesis are too slow to be practical without a catalyst, and protein catalysts hold some advantage over synthetic catalysts, but for reactions that do not occur in living systems there are no natural enzymes. In these circumstances, theoretical protein design followed by directed laboratory evolution can aid in the development of effective artificial enzymes required to drive these chemical transformations[1]. The core question raised by directed evolution is how to achieve the catalytic power of natural enzymes, and thus to inform better initial "theozyme" design. In order to answer this question, we must develop a detailed atomic level picture of the mechanisms of enzymatic reactions at each stage of laboratory evolution. Many enzymatic reactions involve hydrogen transfers, in which a hydrogen atom, proton, or hydride is transferred between molecules. Tunneling can play a key role in these processes since hydrogen is a tunneling-favorable light particle. In this article we study a family of artificial enzymes created to catalyze the Morita-Baylis-Hilman reaction – one for which there is no biologic chemistry. In a previous paper we have

shown the emergence of protein dynamics as a contributor to the mechanism of this process[2]. Here we use related methods to study whether quantum tunneling develops as an important contributor to reaction. The rate determining step for this reaction involves hydrogen transfer, and so it is a natural question, and it poses an interesting intellectual construct: does quantum mechanical tunnelling contribute to activity improvements that emerge during directed evolution? There is absolutely no reason why it should not, but to our knowledge there is no example of this being shown.

While there is no direct experimental measure of the importance of tunneling in a reaction, certain experimental indicators have been used in the enzyme literature to diagnose the likely importance of tunneling to a reaction. The prime one has been Kinetic Isotope Effects (KIE). From pure zero-point considerations one can predict the difference in effective barrier heights seen by a proton and a deuteron, but if tunneling is involved given the exponential effect of mass on tunneling probability, the KIE is thought to be enhanced in the case of tunneling[3]. There is a vast experimental biochemistry literature on this technique, and here we briefly summarize some of the classic work. Cha et al. found that the k_H/k_T ratio in the oxidation of benzyl alcohol to benzaldehyde catalyzed by Yeast Alcohol Dehydrogenase (YADH) was significantly greater than expected in the absence of tunneling[4]. In another work, Grant et al. demonstrated hydrogen tunneling during benzylamine oxidation catalyzed by bovine serum amine oxidase[5]. Further research indicated that mutation in enzymes can expose the presence of tunneling[6,7]. In the study of the oxidation of benzyl alcohol catalyzed by the horse Liver Alcohol Dehydrogenase (LADH), Bahnson et al. found that the reduction in the size of the alcohol binding pocket caused by mutations of the protein results in the appearance of a tunneling effect which was not observed in the wild type of enzyme[6,7]. An extreme example of room temperature tunneling is found in the soybean lipoxygenase system which has KIE's as high as 80 reported[8]. Aromatic Amine Dehydrogenase (AADH) and Methylamine Dehydrogenase (MADH), which catalyze the oxidative deamination of primary amines into aldehydes and ammonia, are notable examples of enzymes that aid to break the C-H bond and demonstrate hydrogen tunneling during this reaction step[9]. The authors demonstrated that KIE for Tryptophan Tryptophyl Quinone (TTQ) reduction by dopamine in AADH is temperature independent, whereas reaction rates are very temperature dependent. Furthermore, they demonstrated that the substrate is influences both KIE and rates.

In this study, we are interested in a C-H substrate bond transferring a proton. An example of the mechanism is shown in Figure 1. This overall proton transfer is subdivided into two proton transfer events. The key residue participating in this reaction example is thought to be glutamic acid.[8] First, glutamic acid plays the role of the hydrogen donor to protonate the O^- of the substrate. Second, glutamic acid is an acceptor of the proton from the broken C-H bond.

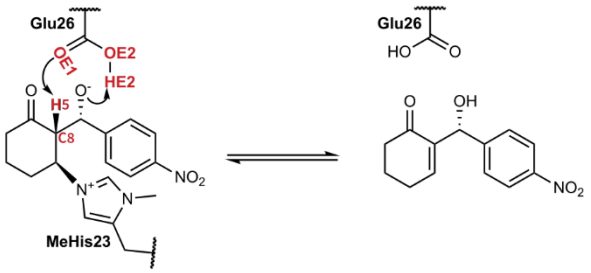

Figure 1. Reaction scheme for the direct protonation mechanism between the N-methylhistidine substrate adduct (Int 2) and the GluH residue in BH1.8. First transfer: HE2 atom of the GluH is transferred to the O^-. Second transfer: H5 of the C8-H5 bond is transferred to the OE1 atom of the Glu residue (possible tunneling).

We find that our results regarding tunneling and barrier height are the same if we include both proton transfers, or only the second, indicating the second transfer must be rate limiting. We use both theoretical and experimental methods to understand the nature of hydrogen transfer in the MBH reaction catalyzed by different variants of an artificial enzyme, drawing on a variety of prior research[2,10,11].

PREVIOUS THEORETICAL STUDIES

A variety of theoretical approaches have been used to aid in the interpretation of experimental observations tied to tunneling. Billeter et al., model the hydride transfer reaction catalyzed by the LADH using hybrid quantum/classical MD approaches for tunneling simulation[12]. The reaction was thought to be electronically adiabatic. Using a multidimensional vibrational wave function[13] representation and the Empirical Valence Bond (EVB) approach[14], the quantum effects of the H nucleus and the electrons were respectively integrated. Free energy profiles were calculated as a function of a collective reaction coordinate analogous to Marcus Theory[15]. The transition state theory rate constant was derived from the free energy profiles and used to calculate the tunneling probability[16].

The Ensemble-Averaged Variational Transition State Theory with Multidimensional Tunneling (EA-VTST-MT) is another method that has been used to include tunneling to the reaction modeling[17,18]. In this method, a system is separated into primary and secondary zones. The potential of mean force (PMF) is then determined by using umbrella sampling MD along a chosen reaction coordinate. The PMF of activation in combination with classical free energy provides the classical free energy of activation. In addition, a quasi-classical approach based on quantum mechanical harmonic vibrational partition functions is used to incorporate the quantized vibrations, such as zero-point energy and thermally induced multidimensional tunneling, in the free energy of activation for atoms from the primary zone. Finally, the ensemble averaging approach can incorporate the free energy shift caused by the secondary zone's motion.

METHODS

We wish to employ an unbiased approach to investigating tunneling with no pre-chosen path and so will use Transition Path Sampling as in previous studies of these designed protein catalysts. The difficulty encountered is TPS is an inherently trajectory-based method. Path integral approaches allow for the treatment of several nuclei in a quantum manner still using trajectory like approaches as opposed to wavefunction methods[19]. One of these techniques, developed by Cao and Voth, is called Centroid Molecular Dynamics (centroid MD)[20]. We have previously given details of the use of this approach in Transition Path Sampling (TPS)[21,22]. Because TPS is an inherently trajectory-based method, path integrals are the natural choice for inclusion of quantum effects in TPS simulations. The primary idea behind this method is to depict the quantum particle as a ring of beads connected by harmonic potentials, and to describe its motion using the motion of the centroid of the beads. A normal mode transformation separates the beads' rapid motion from the centroid's slower motion. The combination of this propagation strategy and the Transition Path Sampling (TPS) method[23,24] allows for an unbiased simulation of the movement of the quantum proton(s) from the reactant to the product state. Because it is an inherently trajectory-based method, we can directly use the free energy methods we previously developed with both classical dynamics and quantum dynamics. Comparison of free energy barriers is then the method by which we assess the importance of tunneling – here it will be manifested by a lower apparent free energy barrier.

The theoretical KIE's are necessarily computed only on the chemical chemical step assuming equivalent preexponential factors in a rate expression.

$$KIE_{theor} = e^{\frac{(\Delta G^D - \Delta G^H)}{RT}} \quad (1)$$

ΔG^D and ΔG^H are the free energy barriers for centroid deuterium and centroid hydrogen calculations, respectively. One assumption made here is that because deuterium is too heavy to tunnel (in most of the cases), the free energy barrier for centroid deuterium calculation should be equal to that of classical hydrogen calculation. This is verified in a specific example given below. (See Results and Discussions section).

All chemicals and biological materials were obtained from commercial suppliers. BH32.12[7] and BH1.8[8] were expressed and purified as previously described. A new procedure was developed to synthesize cyclohex-2-en-1-one-2,6,6-d_3 (2-cyclohexen-1-one-d), which gives 98% deuteration at C8. This is described in the Supporting Information. KIEs were measured under steady state (multiple turnover) conditions using a stopped assay, as described previously.[7,8] Measurements were performed in triplicate, with rates and KIEs reported as the mean ± 1 standard deviation. Relative reaction velocities (V_{rel}) and observed KIEs are given in Table 1, with additional data provided as Supporting Information.

Table 1. KIEs observed and calculated on the enzyme reactions investigated in this study

Protein	Substrate[a]	V_{rel}[b]	KIE_{obs}	KIE_{theor}
BH1.8	4-nitrobenzaldehyde	1.00 ± 0.06	2.04 ± 0.20	14
BH1.8	4-methoxybenzaldehyde	(2.03 ± 0.19) ×10^{-3}	3.39±0.22	4.5
BH32.12	4-nitrobenzaldehyde	(2.88 ± 0.40) ×10^{-2}	2.36 ± 0.30	1

[a]All reactions also included protiated or deuterated 2-cyclohexen-1-one. Reaction conditions are given in Table S1. [b]Observed reaction velocities relative to the BH1.8 reaction with 4-nitrobenzaldehyde and protiated 2-cyclohexen-1-one.

COMPUTATIONAL DETAILS

We focus on the two proteins which showed the highest catalytic activity following directed evolution. The rate-limiting step is thought to comprise of the transfer of two protons: *(i)* hydration of the substrate's O^- and *(ii)* the breaking of the substrate's C-H bond (Figure 1). To explore the tunneling magnitude, the proton of the C-H bond was treated either as a classical particle or approximately as a quantum particle. Two potential pathways for the protons transfer discussed in our earlier study[8] were considered. In one case, the substrate and the appropriate enzyme residue can transfer the protons directly. Another situation requires a water molecule to act as a mediator in these transfers. The final distinction in the examined reactions is the chemical structure of the substrate. Two different substrates reacting with 2 cyclohexen-1-one were proposed based on the experimental work (Table 1).

To model the transition from reactant to product state, we employ transition path sampling. All systems are described within the QM/MM approach - the reaction center (the substrate and a fragment of the protein engaging in the reaction directly or indirectly) is described at the quantum (PM3) level, while the rest of the protein and solvation sphere are described at the molecular mechanics level. In case of BH1.8 protein, the reaction center included the N-methylhistidine substrate adduct and the GluH26 residue, whereas for protein BH32.12, the reaction center included histidine substrate adduct, the Arg124 residue, and one water molecule. All systems were solvated, heated, and equilibrated before running the TPS computations. Our previous study contains all the details on the system setup and TPS simulations[2]. The length of each TPS trajectory was 500 fs. For each system, a set of 200–300 trajectories was obtained.

A window-based sampling procedure was then applied to the representative TPS trajectories to compute the free energy barriers[25]. The free energy barrier is a pathway-dependent value. To ensure that we find representative results, multiple trajectories were employed to calculate free energy values for each system. An appropriate order parameter was selected based on the reaction mechanism. The order parameter describes the proton transfer between the donor and acceptor, but we impose no potential to hold the trajectory to the window, we simply evaluate the populations in each window of a TPS trajectory. The number of windows varies by system and depends on the range of order parameters. The number of windows in this study was ten or fifteen. Each window has approximately 1500-2000 very short trajectories. This enables convergence to be reached. Free energies are obtained from Boltzmann inversion of the populations in each window, and error bars are estimated from standard deviations obtained using bootstrapping analysis.

The quantum proton was represented in terms of centroid molecular dynamics as we previously employed[26]. This proton was described by a centroid with either 8 or 16 beads. The classical and quantum representation of the hydrogen atom is shown in Figures 2(a) and 2(b). A 16 beads test was performed on one of the systems to check the convergence of the results. The centroid propagation timestep was 1 fs, and ten normal mode MD short time steps were done for each of the centroid MD steps. We implement a RESPA propagation method as described in our previous papers[26–28]. The last TPS trajectory from the classical set was used as a starting point for the centroid TPS. For each system, a new set of centroid TPS trajectories was collected. Centroid MD was also used for free energy calculations.

RESULTS AND DISCUSSIONS

We began our investigation with a system that demonstrated the largest classical free energy barrier in our earlier study. This system, known as BH1.8, is a new generation of directed evolution. The protein catalyst of this system has a N-methyl histidine (MeHis) instead of His that was a nucleophile in the earlier versions of the protein and the reactant substrate is either 4-nitrobenzaldehyde or 4-methoxybenzaldehyde. The residue that acts as a proton acceptor after the C-H bond cleavage is glutamic acid. Following the protonation of the substrate's O^-, GluH is deprotonated by transfer to the substrate oxyanion, and the proton of the C-H bond is then transferred directly from the carbon atom to the Glu residue (Figure 1). The order parameter for this system used to chart progress along actual TPS trajectories was the difference between the donor-hydrogen distance (C-H) and the acceptor-hydrogen distance (O-H). The corresponding free energy barrier values and curves calculated using the classical and centroid MD approaches are presented in Table 2 and in Figure 2(c, d). Zero-point energies (ZPE) and the ΔG energies are the two key values that can be extracted from the free energy curves to determine the likelihood of proton tunneling. ZPE is calculated as a difference between the energies of the reactant state (E_{RS}) of the quantum simulation and the classical simulation. ΔG is determined as the difference between the transition state energy (E_{TS}) value and corresponding reactant state energy (E_{RS}) value.

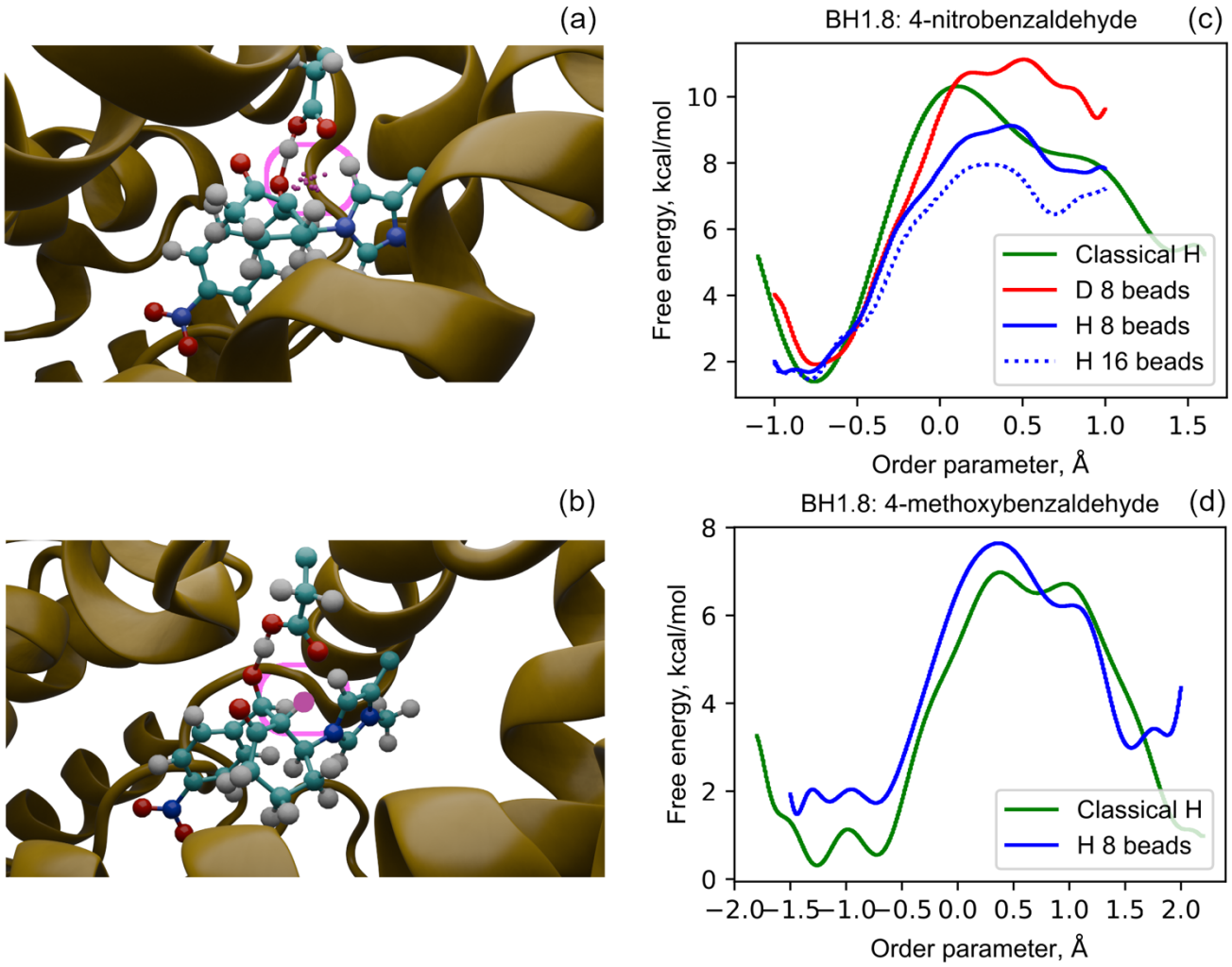

Figure 2. (a) Protein: 1.8 (MeHis); Substrate: 4-nitrobenzaldehyde; Residue: GluH. The transferred proton is presented as 16 beads (in a magenta color box); (b) Protein: BH1.8 (MeHis); Substrate: 4-nitrobenzaldehyde; Residue: GluH. The transferred proton is presented classically (in a magenta color box); (c) Protein: 1.8 (MeHis); Substrate: 4-nitrobenzaldehyde; Residue: GluH. The following free energy profiles are presented: classical simulation (green line), deuterium 16 beads centroid simulation (red line), hydrogen 8 beads centroid simulation (blue line), hydrogen 16 beads centroid simulation (dashed blue line); (d) Protein: 1.8 (MeHis); Substrate: 4-methoxybenzaldehyde; Residue: GluH. The free energy profiles are presented in Figure 2: classical simulation (green line), hydrogen 8 beads centroid simulation (blue line) with the reactant state shown on the left of the curves.

Figure 2c presents an example of the free energy barriers for BH1.8 protein with 4-nitrobenzaldehyde substate. Classical simulation for trajectory # 322 produced an 8.9 kcal/mol barrier, whereas the centroid simulation for trajectory 542 yielded a 7.5 kcal/mol barrier (with 8 beads representation). The drop in free energy barrier height when computed with centroid MD must be ascribed to proton quantum tunnelling. Zero-point energy in the case of 8 beads proton representation is 0.3 kcal/mol. The disparity between the theoretical ZPE of the C-H bond, which is 4 kcal/mol at a stretching frequency of 2900 cm^{-1}, and the obtained ZPE can be explained by two factors. First, TPS calculations are not performed in a vacuum. The C-H bond has a protein environment and a solvation sphere. The second, and most significant, point is that the free energy is calculated along an order parameter that has been carefully selected to best describe the proton transfer. Not just the C-H bond stretch is contained in this order parameter. The precise ZPE value cannot be extracted from the given free energy curve due to these considerations. Finally, the difference in free energies between classical and quantum-8-beads simulations $\Delta(\Delta G)$ is 1.4 kcal/mol. Usually, a value of 1-3 kcal/mol is considered proof of the quantum tunnelling effect[29–33]. The calculated KIE value in this case is 14, which is higher than the experimental result, but still a reasonable value and high enough to confirm the tunnelling mechanism. Thus, we assume that there is a tunnelling contribution in this system.

Table 2. Details of the molecular simulations and free energy barriers for the studied systems

System's specifications	Computational method	Atom (number of beads)	Order parameter, Å	E_{RS}, kcal/mol	ZPE, kcal/mol	E_{TS}, kcal/mol	ΔG (E_{TS}-E_{RS}), kcal/mol
Protein: BH32.12 **Substrate:** 4-nitrobenzaldehyde **Residue:** Arg, H_2O	Classical MD	H5 (0)	d(H5-OH2)	1.7	-	8.3	6.6±0.1
	Centroid MD	H5 (8)	d(H5-OH2)	1.7	0.0	8.5	6.8±0.1
Protein: BH1.8 **Substrate:** 4-nitrobenzaldehyde **Residue:** GluH	Classical MD	H5 (0)	d(CH)-d(OH)	1.4	-	10.3	8.9±0.1
	Centroid MD	H5 (8)	d(CH)-d(OH)	1.7	0.3	9.2	7.5±0.1
Protein: BH1.8 **Substrate:** 4-methoxybenzaldehyde **Residue:** GluH	Classical MD	H5 (0)	d(CH)-d(OH)	0.3	-	7.0	6.7±0.1
	Centroid MD	H5 (8)	d(CH)-d(OH)	1.8	1.5	7.7	5.9±0.1

The entire computation was repeated with deuterium in place of hydrogen to further demonstrate the quantum character of the proton transfer in the system. This test resulted in a barrier of 9.2 kcal/mol for trajectory # 691 (Table 1s in Supporting Information). In the case where only one hydrogen atom can tunnel, we expected to obtain a free energy barrier value for the deuterium case that is equivalent to the classical simulation of the hydrogen transfer. The deuterium test supports the validity of the results. One further test was conducted to confirm that 8 beads are sufficient to describe a proton as a partially quantum particle. In this test, the hydrogen was represented with 16 beads rather than 8 beads (also trajectory # 542). As shown in Figure 2(c), the two corresponding curves (for 8 and 16 beads) are similar in shape, but the curve for 16 beads is slightly lower and gives the ΔG value of 6.4 kcal/mol. It is worth noting here that one free energy calculation contains tens of thousands of MD simulations. To strike a balance between result accuracy and computational costs, it was decided to utilize the 8 beads proton representation for other systems.

We find one significant difference in our free energy results as compared to those we have found in naturally evolved enzymes. The free energy barrier values calculated for different trajectories from the classical and centroid TPS ensembles are shown in Table 3 and Table S1 (Supporting Information), respectively. Three classical, two centroid (hydrogen particle), and three centroid (deuterium particle) trajectories were used to calculate the free energy barriers for BH1.8: 4-nitrobenzaldehyde system. It was found that the free energy barriers varied by 2-3 kcal/mol between various trajectories for each corresponding TPS ensemble. Prior to beginning the TPS procedure, the system was well-equilibrated. A 70 ps MD was carried out with potential energy monitoring to guarantee that the system was in a stable minimum state. Also, the TPS trajectories used for the free energy calculations are 150 or more iterations away from the initial biased trajectory, indicating that they are completely unbiased and decorrelated. The fact that free energy is a path-dependent quantity leads us to think that the TPS ensemble contains trajectories with slightly different paths. We again note that we have never encountered such a result in the study of free energy barriers in naturally occurring enzymes. A comparative analysis was carried out between this system and a system that with a differently substituted substrate: the reaction of BH1.8 with the 4-methoxybenzaldehyde substrate is 35-fold slower than with 4-nitrobenzaldehyde (Table 1). Based on the experimental data, it was proposed that the different rates were caused by the different electronegativity of the $-NO_2$ and $-OCH_3$ groups. In the case of 4-nitrobenzaldehyde substrate (more electronegative group) it is easier to donate a proton (break the C-H bond), which leads to a faster reaction compared to the 4-methoxybenzaldehyde substrate. However, it should be mentioned that the reactive center is a considerable distance away from these groups (Figure 1 shows the location of the $-NO_2$ group). C–H bond frequency analysis (stretching component only) using the wB97M-D3 method for the two substrates (isolated Int2 in vacuum) showed a weaker C–H bond for 4-nitrobenzaldehyde (d(C–H) = 1.162 Å, stretching frequency 2425.5 cm^{-1}) and a stronger C–H bond for 4-methoxybenzylaldehyde (d(C–H) = 1.140 Å, stretching frequency 2534.5 cm^{-1}). This means that the amount of energy required to stretch the C–H bond is 3.47 kcal/mol and 3.62 kcal/mol for 4-nitrobenzaldehyde and 4-methoxybenzylaldehyde, respectively. Given this small difference in stretching frequency, we do not expect the electronegativity factor to have a major impact on the free energy barriers. It means that a detailed analysis of the proton transfer mechanism and the protein dynamics should be done for both systems to determine the cause of the 500-fold rate difference.

Table 3. Free energy barriers and protein dynamics for different classical trajectories of the studied systems

Protein	**Substrate**	**Trajectory #**	**Classical free energy, kcal/mol**	**d (LEU122 – substrate), Å**	**d (PHE45 – GluH), Å**
BH1.8	4-nitrobenzaldehyde	322	8.7±0.2	7.1 - 7.9	6.1 - 6.6
		331	11.0±0.1	6.6 - 7.1	5.6 - 6.5
		392	12.6±0.3	6.3 - 7.6	6.1 - 6.9
	4-methoxybenzalde-hyde	173	6.7±0.1	5.8 - 6.2	4.0 - 4.5
		178	10.6±0.2	5.8 - 6.2	4. - 4.5
		182	9.5±0.1	5.8 - 6.0	4.1 - 4.5
		199	7.2±0.1	5. 5 - 6.9	3.9 - 4.2
		202	7.6±0.2	5. 9 - 7.0	3.8 - 4.1
BH32.12	4-nitrobenzaldehyde	192	9.1±0.1	-	-
		196	6.6±0.1	-	-

To compare the mechanisms of the proton transfers, twenty corresponding distance time series were examined for both systems. Figure 3 (a) and (b) shows an example of the evolution of the OE2-HE2 (corresponding to the first proton transfer) and H5-OE1 (corresponding to the second proton transfer, studied in this paper) distances along the trajectories for the BH1.8: 4-nitrobenzaldehyde and BH1.8: 4-methoxybenzaldehyde, respectively. At first glance, the mechanism of both transfers appears to be the same, however, there is discrepancy in details. In the case of BH1.8: 4-nitrobenzaldehyde, both transfers occur between 305-315 fs, i.e., in 10 fs. After the C-H bond is broken, the proton is captured by the acceptor, and the product state is directly formed. The transition state geometry is clearly defined with the donor-hydrogen distance of around 1.4 Å. In the case of BH1.8: 4-methoxybenzaldehyde, the transition process is stretched in time (between 225 and 295 fs, i.e., 70 fs) and transition state's structure is unclear. The strong hydrogen oscillations between the donor and acceptor are readily seen during the trajectory visualization. The hydrogen returns to the donor after nearly reaching the transition state, and this process is repeated up to 3-4 times. In the transition state region, the donor-hydrogen bond length is around 1.6 Å, which is a bit longer than for the 4-nitrobenzaldehyde substrate and could affect the tunneling contribution. At the same time, the acceptor-hydrogen distance (H5-OE1) for the second studied transfer in the reactant state is larger in the case of BH1.8:4-methoxybenzaldehyde: ~2.6 Å versus 2.0 Å for BH1.8:4-nitrobenzaldehyde. It makes it easier to reach the transition state in the case of BH1.8: 4-nitrobenzaldehyde, which can speed the reaction and lead to a greater contribution from tunneling. As a result, structural differences between two systems cause varied reaction rates. However, the protein in these two systems is identical, raising the question of why structural differences exist. To further study this issue, the structure of the protein surrounding the reactive center was examined.

Some residues in the active site (TRP124, LEU10, LEU87, GLY91, ILE22), were found to show different positions relative to the substrate or GluH acceptor residue. The data are shown in Table 3. The residue LEU122 is located near the para-nitro or para-methoxy group. The time series of the nearest distance between this residue and the O1 or N atom of the substrates were analyzed. The residue is rotated differently in two systems, with the nearest distance in the case of 4-nitrobenzaldehyde being between the CD2 and N atoms and in the case of 4-methoxybenzaldehyde being between the CD1 and O 1 atoms. In addition to this rotation, the LEU122 is ~1 Å closer to the substrate for 4-methoxybenzaldehyde system. A more significant difference is detected in the positions of the PHE45 residue which is close to the GluH acceptor. In addition to the rotational difference of the phenyl groups, the nearest distance between this phenyl group of the PHE45 and the CD atom of the GluH (which is a part of the -COOH group) is ~2-3 Å shorter in the case of 4-methoxybenzaldehyde. At the same time, the phenyl ring approaches the oxygen atoms (of the -COOH group) at a distance of 3 Å during the dynamics, which is close enough to affect the course of the reaction. This analysis shows that although the same protein is used in both systems, its behavior is slightly different. This difference seems to lead to slightly different reaction pathways and, as a result, to different free energy barrier values for different trajectories from one TPS ensemble. It is important to understand here that this BH1.8 protein is a newly created artificial enzyme and compared to natural enzymes that have evolved for thousands of years, this protein has evolved on a benchtop and has not achieved the optimization of a natural enzyme. So, it is quite possible that this protein is not as tuned to guiding the reaction as that of natural enzymes.

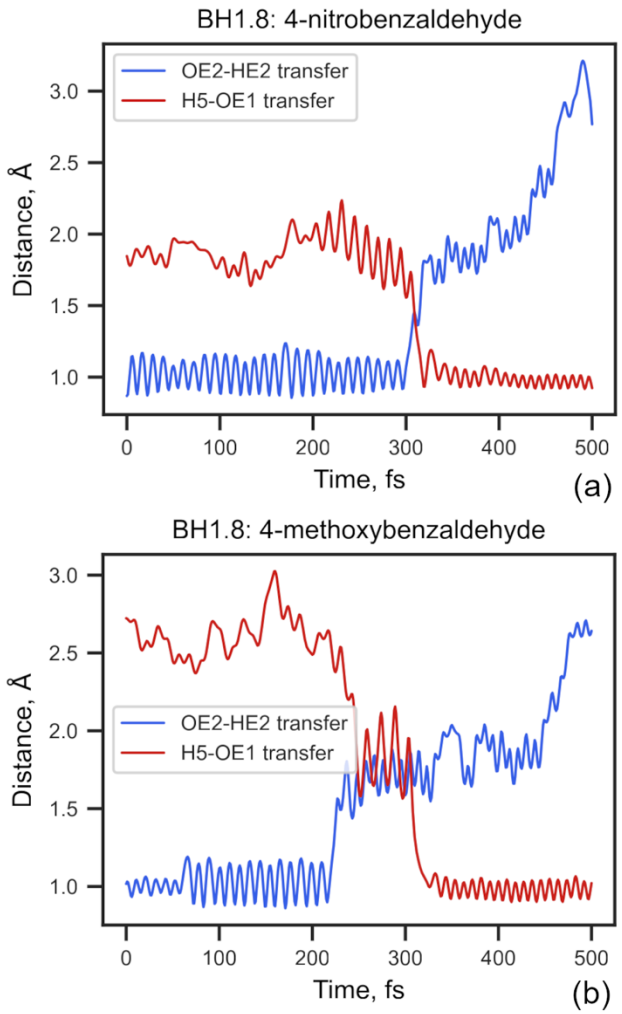

Figure 3. The evolution of the distances corresponding to two hydrogen transfers. First, HE2 proton is transferred from the OE2 to O4 atom (blue line). Second, H5 proton is transferred from C8 to OE1 atom (red line). (a) Protein: BH1.8 (His); Substrate: 4-nitrobenzaldehyde. (b) Protein: BH1.8 (His); Substrate: 4-methoxybenzaldehyde.

The results of the free energy calculations for the BH1.8: 4-methoxybenzaldehyde system are shown in Table 2 and Figure 2(d). It has a free energy barrier of 6.7 kcal/mol. As for the previous system, here we present the results of the lowest free energy barrier (trajectory # 173), since it corresponds to the physically most favored path. Results for other trajectories are given in Table S1 (Supporting Information), and they also show some variation in the free energy barrier values within the TPS ensemble. The quantum-8-beads computation yielded the expected lower ΔG value of 5.9 kcal/mol, which validates a small contribution of the quantum tunnelling mechanism (calculated KIE is 4.5). Both the classical and centroid free energy barriers for BH1.8:4-methoxybenzaldehyde are lower compared to BH1.8:4-nitrobenzaldehyde, although the measured rate is slower. This implies that the reaction rate measured at steady state in the experiment is not completely determined by the chemical step. Protein dynamics have a substantial impact on the reaction rate. The closer proximity of several protein residues to the substrate in BH1.8: 4-methoxybenzaldehyde likely allows for a reduced free energy barrier for the observed chemical step. However, in the case of BH1.8: 4-nitrobenzaldehyde, the protein may perform better overall.

An earlier protein from the directed evolution experiments was the focus of the final stage of this research. The BH32.12 protein, which includes His as a nucleophile and an Arg in place of the Glu found in BH1.8, was chosen because of the low classical energy barrier observed in prior simulations. The substrate of this system is 4-nitrobenzaldehyde. The mechanism of the reaction in this case appears to be water mediated. It means that the transfer of the proton happens between the C-H bond of the substrate and the newly formed OH^- particle (after protonation of the O^- of the substrate). The water molecule is constantly moving relative to the substrate (approaching or moving away from the C-H bond) that means the order parameter must be changed in this case to exclude the contribution of this movement to the free energy profile. The order parameter for this system is the distance between the hydrogen of the C-H bond and the oxygen atom of the OH^- ion.

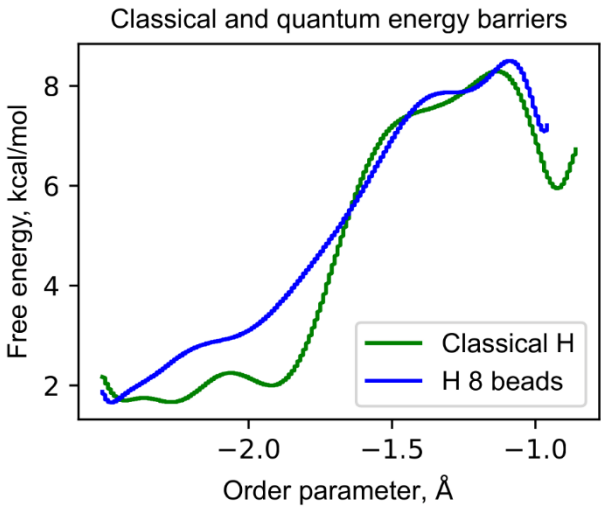

Figure 4. Protein: BH32.12 (His); Substrate: 4-nitrobenzaldehyde; Residue: Arg; 1 water molecule. The following free energy profiles are presented: classical simulation (green line), hydrogen 8 beads centroid simulation (blue line).

Table 2 and Figure 4 show the free energy values and profiles for the BH32.12 protein. We can observe that this system differs from the previous two. The free energy barriers for the classical and quantum-8-beads simulations are essentially identical, measuring 6.6 and 6.8 kcal/mol, respectively. The reactant state energies are likewise identical, at 1.7 kcal/mol, indicating no ZPE in these calculations. The lack of zero-point energy is explained by a change in the order parameter, which in this case does not contain a C-H bond at all, but overall, the classical barrier is low enough to obviate the presence of quantum tunnelling in the reaction. The absence of a quantum tunnelling, along with a, what we can infer to be less rapid conformational change necessary for product production results in a slower chemical reaction rate (V_{rel} ~500-fold slower than for BH1.8), as shown in Table 1.

CONCLUSIONS

The possibility of proton quantum tunneling during C-H bond breakage was studied by experimental and theoretical investigations of three different MBH reaction systems. The main conclusion is that, unsurprisingly, tunneling happens when the barrier is high enough to allow it to contribute significantly to the overall transmission and not needed when the chemical barrier is low. (We again note that we are only able to study the chemical rate in this work – not the overall rate of enzyme turnover. An interesting fact about all the systems is that the height of free energy barrier for all the systems for the hydrogen transfer during the C-H bond cleavage is always around 7 kcal/mol. However, the nature of this transfer can be different, whether classical or quantum. Based on all the experimental and theoretical findings, we can list the factors that can influence the chemical rate of the C-H bond cleavage step of the MBH reaction. The BH32.12 protein showed a lower chemical rate. The same BH1.8 protein functions differently with different substrates. In addition, some variations in protein dynamics result in a variety of potential paths for the studied chemical step. This, in turn, slightly effects the apparent height of the free energy barrier. A chemical reaction proceeds more quickly if the C-H bond is more easily broken. As previously demonstrated, the intricacies of the proton transfer process, namely the existence or absence of strong oscillations of the proton between the donor and acceptor, are also significant. These oscillations slow the chemical reaction. Due to the complexity of protein catalyst function, experimentally measured steady-state reaction rates and KIEs cannot be directly related to the results of theoretical calculations, and except in extreme cases, do not always report directly on quantum tunneling effects.

SUPPORTING INFORMATION

Computational methods, Table S1, Chemical Synthesis, Table S1, Figures S1, S2, S3, NMR Spectra

AUTHOR INFORMATION

Corresponding Author

*Professor Steven D. Schwartz - Department of Chemistry and Biochemistry, University of Arizona, 1306 E University Blvd, Tucson, Arizona 85721, United States;
https:/orcid.org/0000-0002-0308-1059;
Email: sschwartz@arizona.edu

Author Contributions

The manuscript was written through contributions of all authors. All authors have given approval to the final version of the manuscript.

Notes

The authors declare no competing financial interest.

Data Availability Statement

All data supporting this study are provided in the supporting information accompanying this paper.

ACKNOWLEDGMENT

SDS acknowledges funding from the NIH through grant number GM145213 and the NSF through grant number MCB-2244981. We also acknowledge funding from the BBSRC through grant: BB/X000974/1.

Professor Dimitri Antoniou is acknowledged for constructive discussions.

ABBREVIATIONS

MBH reaction Morita-Baylis-Hillman; MD molecular dynamics; TPS transition path sampling; YADH yeast alcohol Dehydrogenase; LADH liver alcohol Dehydrogenase; SBL soybean lipoxygenase; KIE kinetic isotope effect; EVB empirical valence bond; EA-VTST-MT ensemble-averaged variational transition state theory with multidimensional tunneling; PMF potential of mean force; ZPE zero-point energy; RS reactant state, TS transition state, PS product state

REFERENCES

(1) Lovelock, S. L.; Crawshaw, R.; Basler, S.; Levy, C.; Baker, D.; Hilvert, D.; Green, A. P. The Road to Fully Programmable Protein Catalysis. *Nature* **2022**, *606* (7912), 49–58. https://doi.org/10.1038/s41586-022-04456-z.

(2) Balasubramani, S. G.; Korchagina, K.; Schwartz, S. Transition Path Sampling Study of Engineered Enzymes That Catalyze the Morita–Baylis–Hillman Reaction: Why Is Enzyme Design so Difficult? *J. Chem. Inf. Model.* **2024**, *64* (6), 2101–2111. https://doi.org/10.1021/acs.jcim.4c00045.

(3) Johannissen, L. O.; Iorgu, A. I.; Scrutton, N. S.; Hay, S. What Are the Signatures of Tunnelling in Enzyme-Catalysed Reactions? *Faraday Discuss.* **2020**, *221*, 367–378. https://doi.org/10.1039/C9FD00044E.

(4) Cha, Y.; Murray, C. J.; Klinman, J. P. Hydrogen Tunneling in Enzyme Reactions. *Science* **1989**, *243* (4896), 1325–1330. https://doi.org/10.1126/science.2646716.

(5) Grant, K. L.; Klinman, J. P. Evidence That Both Protium and Deuterium Undergo Significant Tunneling in the Reaction Catalyzed by Bovine Serum Amine Oxidase. *Biochemistry* **1989**, *28* (16), 6597–6605. https://doi.org/10.1021/bi00442a010.

(6) Bahnson, B. J.; Park, D. H.; Kim, K.; Plapp, B. V.; Klinman, J. P. Unmasking of Hydrogen Tunneling in the Horse Liver Alcohol Dehydrogenase Reaction by Site-Directed Mutagenesis. *Biochemistry* **1993**, *32* (21), 5503–5507. https://doi.org/10.1021/bi00072a003.

(7) Bahnson, B. J.; Colby, T. D.; Chin, J. K.; Goldstein, B. M.; Klinman, J. P. A Link between Protein Structure and Enzyme Catalyzed Hydrogen Tunneling. *Proc. Natl. Acad. Sci. U.S.A.* **1997**, *94* (24), 12797–12802. https://doi.org/10.1073/pnas.94.24.12797.

(8) Jonsson, T.; Glickman, M. H.; Sun, S.; Klinman, J. P. Experimental Evidence for Extensive Tunneling of Hydrogen in the Lipoxygenase Reaction: Implications for Enzyme Catalysis. *J. Am. Chem. Soc.* **1996**, *118* (42), 10319–10320. https://doi.org/10.1021/ja961827p.

(9) Basran, J.; Patel, S.; Sutcliffe, M. J.; Scrutton, N. S. Importance of Barrier Shape in Enzyme-Catalyzed Reactions. *Journal of Biological Chemistry* **2001**, *276* (9), 6234–6242. https://doi.org/10.1074/jbc.M008141200.

(10) Crawshaw, R.; Crossley, A. E.; Johannissen, L.; Burke, A. J.; Hay, S.; Levy, C.; Baker, D.; Lovelock, S. L.; Green, A. P. Engineering an Efficient and Enantioselective Enzyme for the Morita–Baylis–Hillman Reaction. *Nat. Chem.* **2022**, *14* (3), 313–320. https://doi.org/10.1038/s41557-021-00833-9.

(11) Hutton, A. E.; Foster, J.; Crawshaw, R.; Hardy, F. J.; Johannissen, L. O.; Lister, T. M.; Gérard, E. F.; Birch-Price, Z.; Obexer, R.; Hay, S. et al. A Non-Canonical Nucleophile Unlocks a New Mechanistic Pathway in a Designed Enzyme. *Nat Commun* **2024**, *15* (1), 1956. https://doi.org/10.1038/s41467-024-46123-z.

(12) Billeter, S. R.; Webb, S. P.; Agarwal, P. K.; Iordanov, T.; Hammes-Schiffer, S. Hydride Transfer in Liver Alcohol Dehydrogenase: Quantum Dynamics, Kinetic Isotope Effects, and Role of Enzyme Motion. *J. Am. Chem. Soc.* **2001**, *123* (45), 11262–11272. https://doi.org/10.1021/ja011384b.

(13) Webb, S. P.; Hammes-Schiffer, S. Fourier Grid Hamiltonian Multiconfigurational Self-Consistent-Field: A Method to Calculate Multidimensional Hydrogen Vibrational Wavefunctions. *The Journal of Chemical Physics* **2000**, *113* (13), 5214–5227. https://doi.org/10.1063/1.1289528.

(14) Warshel, A. *Computer Modeling of Chemical Reactions in Enzymes and Solutions.*; John Wiley & Sons, Inc.: New York, 1991.

(15) Marcus, R. A. Chemical and Electrochemical Electron-Transfer Theory. *Annu. Rev. Phys. Chem.* **1964**, *15*, 155.

(16) Wigner, E. On the Quantum Correction For Thermodynamic Equilibrium. *Phys. Rev.* **1932**, *40* (5), 749–759. https://doi.org/10.1103/PhysRev.40.749.

(17) Pu, J.; Gao, J.; Truhlar, D. G. Multidimensional Tunneling, Recrossing, and the Transmission Coefficient for Enzymatic Reactions. *Chem. Rev.* **2006**, *106* (8), 3140–3169. https://doi.org/10.1021/cr050308e.

(18) Alhambra, C.; Corchado, J.; Sánchez, M. L.; Garcia-Viloca, M.; Gao, J.; Truhlar, D. G. Canonical Variational Theory for Enzyme Kinetics with the Protein Mean Force and Multidimensional Quantum Mechanical Tunneling Dynamics. Theory and Application to Liver Alcohol Dehydrogenase. *J. Phys. Chem. B* **2001**, *105* (45), 11326–11340. https://doi.org/10.1021/jp0120312.

(19) Feynman, R. P.; Hibbs, A. R. *Quantum Mechanics and Path Integrals*; McGraw-Hill: New York, 1965.

(20) Cao, J.; Voth, G. A. The Formulation of Quantum Statistical Mechanics Based on the Feynman Path Centroid Density. IV. Algorithms for Centroid Molecular Dynamics. *The Journal of Chemical Physics* **1994**, *101* (7), 6168–6183. https://doi.org/10.1063/1.468399.

(21) Antoniou, D.; Schwartz, S. D. The Stochastic Separatrix and the Reaction Coordinate for Complex Systems. *The Journal of Chemical Physics* **2009**, *130* (15), 151103. https://doi.org/10.1063/1.3123162.

(22) Dzierlenga, M. W.; Varga, M. J.; Schwartz, S. D. Path Sampling Methods for Enzymatic Quantum Particle Transfer Reactions. In *Methods in Enzymology*; Elsevier, 2016; Vol. 578, pp 21–43. https://doi.org/10.1016/bs.mie.2016.05.028.

(23) Bolhuis, P. G.; Dellago, C. Practical and Conceptual Path Sampling Issues. *Eur. Phys. J. Spec. Top.* **2015**, *224* (12), 2409–2427. https://doi.org/10.1140/epjst/e2015-02419-6.

(24) Bolhuis, P. G.; Swenson, D. W. H. Transition Path Sampling as Markov Chain Monte Carlo of Trajectories: Recent Algorithms, Software, Applications, and Future Outlook. *Advcd Theory and Sims* **2021**, *4* (4), 2000237. https://doi.org/10.1002/adts.202000237.

(25) Balasubramani, S. G.; Schwartz, S. D. Transition Path Sampling Based Calculations of Free Energies for Enzymatic Reactions: The Case of Human Methionine Adenosyl Transferase and *Plasmodium Vivax* Adenosine Deaminase. *J. Phys. Chem. B* **2022**, *126* (29), 5413–5420. https://doi.org/10.1021/acs.jpcb.2c03251.
(26) Antoniou, D.; Schwartz, S. D. Approximate Inclusion of Quantum Effects in Transition Path Sampling. *The Journal of Chemical Physics* **2009**, *131* (22), 224111. https://doi.org/10.1063/1.3272793.
(27) Tuckerman, M.; Berne, B. J.; Martyna, G. J. Reversible Multiple Time Scale Molecular Dynamics. *The Journal of Chemical Physics* **1992**, *97* (3), 1990–2001. https://doi.org/10.1063/1.463137.
(28) Tuckerman, M. E.; Berne, B. J.; Rossi, A. Molecular Dynamics Algorithm for Multiple Time Scales: Systems with Disparate Masses. *The Journal of Chemical Physics* **1991**, *94* (2), 1465–1469. https://doi.org/10.1063/1.460004.
(29) Delgado, M.; Görlich, S.; Longbotham, J. E.; Scrutton, N. S.; Hay, S.; Moliner, V.; Tuñón, I. Convergence of Theory and Experiment on the Role of Preorganization, Quantum Tunneling, and Enzyme Motions into Flavoenzyme-Catalyzed Hydride Transfer. *ACS Catal.* **2017**, *7* (5), 3190–3198. https://doi.org/10.1021/acscatal.7b00201.
(30) Pang, J.; Hay, S.; Scrutton, N. S.; Sutcliffe, M. J. Deep Tunneling Dominates the Biologically Important Hydride Transfer Reaction from NADH to FMN in Morphinone Reductase. *J. Am. Chem. Soc.* **2008**, *130* (22), 7092–7097. https://doi.org/10.1021/ja800471f.
(31) Faulder, P. F.; Tresadern, G.; Chohan, K. K.; Scrutton, N. S.; Sutcliffe, M. J.; Hillier, I. H.; Burton, N. A. QM/MM Studies Show Substantial Tunneling for the Hydrogen-Transfer Reaction in Methylamine Dehydrogenase. *J. Am. Chem. Soc.* **2001**, *123* (35), 8604–8605. https://doi.org/10.1021/ja016219a.
(32) Ranaghan, K. E.; Masgrau, L.; Scrutton, N. S.; Sutcliffe, M. J.; Mulholland, A. J. Analysis of Classical and Quantum Paths for Deprotonation of Methylamine by Methylamine Dehydrogenase. *ChemPhysChem* **2007**, *8* (12), 1816–1835. https://doi.org/10.1002/cphc.200700143.
(33) Tejero, I.; Garcia-Viloca, M.; González-Lafont, À.; Lluch, J. M.; York, D. M. Enzyme Dynamics and Tunneling Enhanced by Compression in the Hydrogen Abstraction Catalyzed by Soybean Lipoxygenase-1. *J. Phys. Chem. B* **2006**, *110* (48), 24708–24719. https://doi.org/10.1021/jp066263i.